

# Arrival-time structure of the time-averaged ambient noise cross-correlation function in an oceanic waveguide<sup>a)</sup>

Karim G. Sabra, Philippe Roux, and W. A. Kuperman<sup>b)</sup>

*Marine Physical Laboratory, Scripps Institution of Oceanography, La Jolla, California 92103-0238*

(Received 23 February 2004; revised 29 October 2004; accepted 29 October 2004)

Coherent deterministic arrival times can be extracted from the derivative of the time-averaged ambient noise cross-correlation function between two receivers. These coherent arrival times are related to those of the time-domain Green's function between these two receivers and have been observed experimentally in various environments and frequency range of interest (e.g., in ultrasonics, seismology, or underwater acoustics). This nonintuitive result can be demonstrated based on a simple time-domain image formulation of the noise cross-correlation function, for a uniform distribution of noise sources in a Pekeris waveguide. This image formulation determines the influence of the noise-source distribution (in range and depth) as well as the dependence on the receiver bandwidth for the arrival-time structure of the derivative of the cross-correlation function. These results are compared with previously derived formulations of the ambient noise cross-correlation function. Practical implications of these results for sea experiments are also discussed. © 2005 Acoustical Society of America. [DOI: 10.1121/1.1835507]

PACS numbers: 43.30.Nb, 43.30.Wi, 43.20.Bi [DRD]

Pages: 164–174

## I. INTRODUCTION

The acoustic time-domain Green's function (TDGF) fully determines the acoustic propagation timing between two points. The TDGF is usually characterized by broadcasting a known signal shape from one point and determining its modifications (in the frequency- or the time domain), after propagation through the medium, from the recorded signal at the other point. However, it has recently been experimentally demonstrated<sup>1,2</sup> that by cross correlating ambient noise recordings from two distinct locations, it is possible to build an estimate of the TDGF between these two receivers. Earlier conjectures of this result were also formulated.<sup>3,4</sup> Successful extraction of TDGF estimates between two points has recently been achieved experimentally using acoustic ambient noise measurements *only* for specific environments and measured frequency. For instance (1) ultrasonic, using measurements of diffuse noise fields;<sup>1,2</sup> (2) seismology, using fully diffuse ambient seismic noise;<sup>5</sup> (3) helioseismology<sup>4</sup> using passive solar Dopplergrams recorded by the Michelson Doppler imager; or (4) underwater acoustics using recording of sea surface generated ambient noise.<sup>6</sup> In addition, different techniques for constructing TDGF estimates, still based on cross correlations, have also been proposed. These other techniques do not directly use ambient noise measurements but instead distributed sources in the propagating medium in order to create a “sufficiently” diffuse acoustic field in this medium. Examples are (1) an ultrasonic scattering medium using several controlled sources;<sup>7,8</sup> (2) in seismology<sup>9</sup> using the diffuse coda of identifiable seismic events; or (3) in an underwater waveguide using controlled secondary sound sources distributed in the water column.<sup>10</sup>

Even if the ambient noise cross-correlation technique is

applied in a different type of environment, the underlying physics relies on the same fact: when using ambient noise measurements, the deterministic coherent wavefronts extracted from time-averaged cross correlations correspond to residual coherent noise between the receivers. This small coherent component of the ambient noise field is buried in the spatially and temporally incoherent field produced by the whole noise source distribution, but emerges after time averaging from those correlations that contain noise sources whose acoustic path passes through both receivers. Thus, these coherent wavefronts yield an estimate of the arrival-time structure of the TDGF. A sufficiently long time-averaging interval (as long as environmental changes do not modify the acoustic propagation paths) and a spatially homogeneous noise distribution help in estimating the arrival-time structure of the TDGF from this correlation process.<sup>6</sup> The differences between the various TDGF estimates (or coherent wavefronts) obtained experimentally using the ambient noise cross-correlations technique in specific environments are linked to the spatio-temporal statistics of the noise sources. Indeed, the amplitudes of the individual extracted coherent wavefronts are shaded by the directionality of the noise sources and their spatial distribution,<sup>6,7</sup> and more frequent random noise events accelerate the emergence of the TDGF estimates from the ambient noise cross correlations.

In a complex environment with boundaries (e.g., oceanic waveguides, ultrasonic cavities), the emergence of an estimate of the TDGF from the long-term correlation of ambient noise recordings was demonstrated experimentally<sup>1–6</sup> but appears at first glance to be a nonintuitive conjecture. This result has been demonstrated theoretically in a cavity using a normal-mode formulation.<sup>1,2</sup> Furthermore, a stationary phase derivation has been proposed to explain the extraction of the ballistic Green's function in seismology from the correlation of multiply scattered waves in a free-space medium with embedded scatterers uniformly distributed.<sup>11</sup> Relationships

<sup>a)</sup>Portions of this work were presented at the 147th ASA meeting, Austin, TX, Nov. 2003.

<sup>b)</sup>Electronic mail: ksabra@mpl.ucsd.edu

between the cross correlation of the transmission response with the reflection response were also derived for an inhomogeneous elastic media.<sup>12</sup> The central result of this article is a demonstration of this conjecture using a straightforward application (though geometrically intricate) of the method of images for a uniform distribution of noise sources in an oceanic waveguide. This method can also be applied to other environments with plane boundaries (for instance in seismology<sup>11</sup>). The main goal of this article is to relate the arrival times ( $\tau$ ) of the time-averaged noise cross-correlation function (NCF)  $C_{1,2}(\tau)$  between the two receivers (i.e., the asymptotic limit of the NCF after a long time-averaging interval) to the arrival times of the TDGF between these two receivers by using a stationary phase condition. In addition, this article provides an explanation for the amplitude shading of the individual extracted coherent wavefronts, as predicted by previous normal-mode formulations<sup>13–15</sup> and also observed experimentally in the ocean:<sup>6</sup> this shading is related to the particular geometric distribution of sea-surface noise sources (which induce a dipole effect when the noise sources are located close to the ocean surface).

Previous detailed analysis of the sources of ocean noise<sup>16–18</sup> (natural and manmade) indicates that high-frequency ocean noise (above several hundred hertz) is not influenced by shipping noise, and is well approximated by a homogeneous spatial distribution of random surface noise sources, with known statistics.<sup>13,19</sup> Thus, this article will focus on high-frequency oceanic ambient noise. In this paper, the case of a simple Pekeris waveguide<sup>20</sup> is studied, for which a simple formulation of the TDGF exists using the image theory: the TDGF between two points can be expressed as a sum of free-space travel times from each of the images of one of these points to the other one.<sup>20</sup> This image formulation is an exact solution of the wave equation for an isospeed and range-independent environment, yet it is analytically simple. It also easily includes the near-field propagation effects for noise sources close to the receivers. The resulting image formulation for the NCF  $C_{1,2}(\tau)$  can be reduced to previous normal-mode formulations<sup>13–15</sup> or ray formulations<sup>21</sup> of the NCF for range-independent environments. From this simple model it follows: (1) that only noise sources located in the endfire direction of the two receivers contribute to the NCF; (2) which among these endfire noise sources actually contributes to a given arrival-time  $\tau$  of  $C_{1,2}(\tau)$ ; and (3) how the arrival times of the NCF depend on the depth of these noise sources. This simple image formulation of the NCF explains the basic physics of this noise cross-correlation process, and should provide an upper-bound estimate for the performance of this noise cross-correlation process in the case of more complex oceanic waveguides.

This paper is divided into three sections. In Sec. II, a simple model of the sea-surface-generated ambient noise is discussed and closed-form analytical results for the NCF,  $C_{1,2}(\tau)$ , are developed for this model. Here, the effects of the noise source depths and the influence of the bandwidth of the two receiving transducers on the time-delay structure of the measured NCF are also investigated. In Sec. III, the issues associated with a field experiment are discussed, nota-

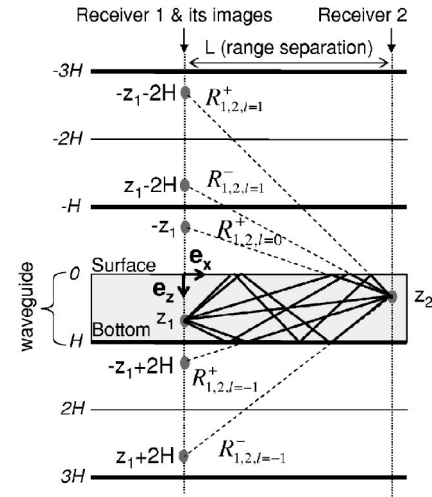


FIG. 1. Superposition of free-space propagations paths ( $R_{1,2,l}^-$  and  $R_{1,2,l}^+$ , displayed in dashed lines) for the first five image sources solutions ( $|l| \leq 1$ ) in an ideal waveguide (depth  $H$ ), between a source located at  $(0,0,z_1)$  and a receiver located at  $(L,0,z_2)$ , as defined in Eq. (1) and Eq. (2). The corresponding physical propagation paths are indicated in plain lines in the waveguide. The various depths of each image and of the two receivers are also displayed.

ably the choice of the length of the correlation time window. Section IV summarizes the findings and conclusions drawn from this study.

## II. TIME-DOMAIN FORMULATION OF THE AMBIENT NOISE CROSS CORRELATION

### A. Surface noise model

At frequencies above several hundred hertz, ambient noise is mostly generated at the ocean's surface.<sup>12,17,22–24</sup> A simple model for the surface-generated ambient noise field<sup>13,19,25–27</sup> is a random distribution, in space and time, of individual point noise sources located in a plane lying beneath the sea surface at a constant depth  $z_s$ . The signal recorded at the two receivers locations from a single random noise source is fully determined by the TDGF for the oceanic waveguide of interest, between this random source and the receivers. The superposition of these random pulses from many noise sources, at a receiver location, produces the measured surface-generated ambient noise.

### B. Image formulation of the ambient noise cross correlation

We start with the time-domain representation of the acoustic pressure field from an impulse point source, based on the method of images,<sup>28</sup> in a isovelocity 3D oceanic waveguide (with a speed of sound  $c_0$ ), of depth  $H$ , bounded above by a pressure-release surface and below by a semi-infinite bottom layer which reduces the pressure amplitude by a reflection coefficient  $V_b$  (see Fig. 1).  $V_b$  is a function of the ray grazing angle and can be determined by the geoacoustic properties of the bottom.<sup>28</sup> Furthermore, volume attenuation is included by adding an imaginary component to the speed of sound<sup>20</sup> ( $c = c_0 - ic_i$ ). For the Cartesian coordinate system ( $\mathbf{e}_x, \mathbf{e}_y, \mathbf{e}_z$ ) defined in Fig. 1, the depth axes,  $\mathbf{e}_z$ , starts from the surface and points downward. The radial vec-

tor in the horizontal plane is  $\mathbf{r} = x\mathbf{e}_x + y\mathbf{e}_y$ , and the horizontal axis originates at the first receiver location ( $x_1=0, y_1=0, z_1$ ). The second receiver is located at ( $x_2=L, y_2=0, z_2$ ), where  $L>0$  by hypothesis. The finite frequency bandwidth of the recordings is  $[\omega_1, \omega_2]$ . To simplify notation, the negative part of the frequency spectrum of the TDGF is ignored. The bandlimited TDGF between the two sensors,  $G(\mathbf{r}_1, z_1, \mathbf{r}_2, z_2; t)$ , can then be expressed as<sup>28</sup>

$$G(\mathbf{r}_1, z_1, \mathbf{r}_2, z_2; t) = \int_{\omega_1}^{\omega_2} \frac{d\omega}{2\pi} \sum_{l=-\infty}^{l=+\infty} (-1)^{|l|} |V_b^l| \left( \frac{e^{i\omega(t-R_{1,2,l}^-/c_0)} \cdot e^{-\omega R_{1,2,l}^- c_i/c_0^2}}{R_{1,2,l}^-} - \frac{e^{i\omega(t-R_{1,2,l}^+/c_0)} \cdot e^{-\omega R_{1,2,l}^+ c_i/c_0^2}}{R_{1,2,l}^+} \right), \quad (1)$$

where  $R_{1,2,l}^-$  and  $R_{1,2,l}^+$  are the free-space distances between the  $l$ th-order image (the third index  $l$  is an integer) of receiver 1 (represented by the first index) and receiver 2 (represented by the second index)

$$\begin{aligned} R_{1,2,l}^- &= \sqrt{(|\mathbf{r}_2 - \mathbf{r}_1|)^2 + (z_2 - z_1 + 2lH)^2} \\ &= \sqrt{L^2 + (z_2 - z_1 + 2lH)^2}, \\ R_{1,2,l}^+ &= \sqrt{(|\mathbf{r}_2 - \mathbf{r}_1|)^2 + (z_2 + z_1 + 2lH)^2} \\ &= \sqrt{L^2 + (z_2 + z_1 + 2lH)^2}. \end{aligned} \quad (2)$$

This notation for the free-space distances  $R$  associated with the image theorem (here,  $R_{1,2,l}^-$  and  $R_{1,2,l}^+$ ) will be used consistently throughout the remainder of this paper: the first index (here 1) corresponds to the source location, the second index (here 2) to the receiver location, and the third index (here  $l$ ) to the source-image order. The exponent (+ or -) indicates, respectively, that the sum ( $z_2 + z_1$ ) or difference ( $z_2 - z_1$ ) of source/receiver depths is used. Figure 1 represents the geometric interpretation of the image theorem for the two receivers. Thus, in Eq. (1), the arrival times of the TDGF correspond to the free-space travel times from each individual images of receiver 1 to receiver 2. For infinite bandwidth (i.e.,  $[\omega_1, \omega_2] = [-\infty, +\infty]$ ) and in the limit of no volume attenuation (i.e.,  $c_i=0$ ), the previous time-domain formulation reduces to

$$G(\mathbf{r}_2, z_2, \mathbf{r}_1, z_1; t)^{inf} = \sum_{l=-\infty}^{l=+\infty} (-1)^{|l|} |V_b^l| \left( \frac{\delta(t-R_{1,2,l}^-/c_0)}{R_{1,2,l}^-} - \frac{\delta(t-R_{1,2,l}^+/c_0)}{R_{1,2,l}^+} \right). \quad (3)$$

In this 3D oceanic waveguide, the noise source distribution is modeled as an infinite 2D plane sheet of monopole impulse sources located at  $(\mathbf{r}_s = x_s \mathbf{e}_x + y_s \mathbf{e}_y, z_s)$ , where  $z_s$  is a constant. In the absence of attenuation in the ocean, the resulting power of the recording ambient noise field would be infinite. In practice, the contribution of the noise sources is limited in range due to bottom absorption and volume attenuation. In this model, each noise source broadcasts, at a random time  $t_s$ , an impulse of amplitude  $S(\mathbf{r}_s; t_s)$ . The signal recorded at the two receivers, locations, from a single ran-

dom source, represented by a delta function in space and time, is fully determined by the TDGF for the oceanic waveguide of interest, between this source and the receivers.<sup>13,19,25</sup> The time-domain recorded signals at the two receivers,  $P(\mathbf{r}_s, z_s, \mathbf{r}_k, z_k; t)$ ,  $k=1, 2$ , are obtained by summing over all the impulse noise sources contributions,<sup>28</sup> using Eq. (1) for the Green's function between each noise source and the receivers  $G(\mathbf{r}_s, z_s, \mathbf{r}_k, z_k; t-t_s)$  for  $k=1, 2$

$$P(\mathbf{r}_s, z_s, \mathbf{r}_k, z_k; t) = \int_{-\infty}^{+\infty} d\mathbf{r}_s \int_{-\infty}^{+\infty} dt_s S(\mathbf{r}_s; t_s) G(\mathbf{r}_s, z_s, \mathbf{r}_k, z_k; t-t_s). \quad (4)$$

In a stationary medium, the temporal NCF,  $C_{1,2}(\tau)$ , between the signals recorded by both receivers is defined as

$$C_{1,2}(\tau) = \int_{-\infty}^{+\infty} dt P(\mathbf{r}_s, z_s, \mathbf{r}_1, z_1; t) P(\mathbf{r}_s, z_s, \mathbf{r}_2, z_2; t+\tau). \quad (5)$$

These random impulse noise sources have a white frequency spectrum, which does not represent the physical frequency spectrum of the sound pulse generated from breaking waves.<sup>22,23,25</sup> However, if the pulses induced by the breaking events are assumed to be identical on average, the source spectrum can be factored out of the spectrum of the received signal. Thus, the NCF is independent of the source spectrum when normalized by the energy of the recorded signals at each receiver location.<sup>26</sup>

In practice, the NCF is constructed from ensemble averages, denoted by  $\langle \rangle$ , over realizations of the noise source amplitude  $S(\mathbf{r}_s; t_s)$ . We assume that the random impulse noise sources have the same amplitude  $Q$  ( $\text{Pa m}^{3/2} \text{s}$ ), have a creation rate<sup>29</sup>  $\nu$  ( $\text{m}^{-2} \text{s}^{-1}$ ) per unit time per surface area, and are temporally and spatially incoherent<sup>13</sup> in the limit of infinite recording time and infinite bandwidth (due to the impulsive nature of the sources); then

$$\langle S(\mathbf{r}_s; t_s) S(\mathbf{r}_{s'}; t_{s'}) \rangle = 2\nu Q^2 \delta(\mathbf{r}_{s'} - \mathbf{r}_s) \cdot \delta(t_{s'} - t_s). \quad (6)$$

Empirical relations between the surface wind speed and the spatial and temporal statistics of breaking waves are available,<sup>30</sup> and can be used to provide estimates of the parameters  $\nu$  and  $Q$  for given sea-state conditions. Since the noise sources are assumed to be uncorrelated after ensemble averaging [see Eq. (6)], only the correlations between the arrival times produced by the images of the same noise source will contribute to the arrival times of the NCF. Thus, using Eqs. (1), (2), (4)–(6), the NCF can be expressed—after simplification—as a sum of four cross terms

$$C_{1,2}(\tau) = \Delta_{1,2}^{-,-} - \Delta_{1,2}^{+,-} - \Delta_{1,2}^{-,+} + \Delta_{1,2}^{+,+}, \quad (7)$$

where

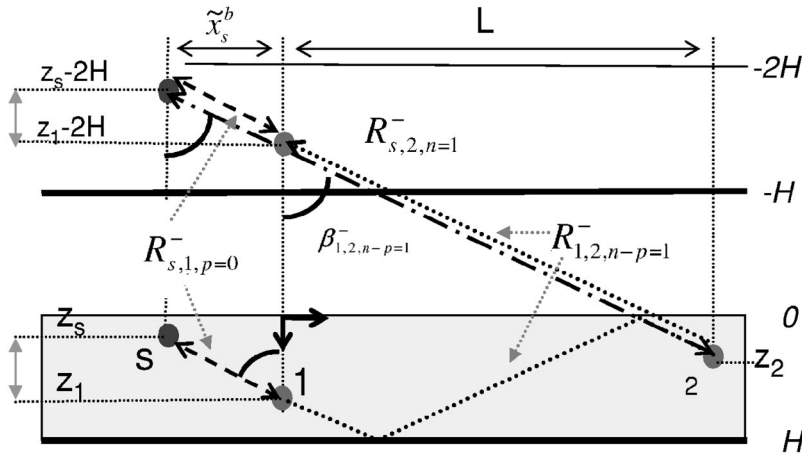


FIG. 2. Geometric construction of the location of the noise source corresponding to the first solution of the stationary phase conditions  $\tilde{\mathbf{r}}_s^b = (\tilde{x}_s^b, \tilde{y}_s^b = 0)$ , for  $n=1$  and  $p=0$  [see Eq. (12) and Eq. (13)]. Note the alignment between the noise source image [at depth  $z_s - 2(n-p)H = z_s - 2H$ ], the image of receiver 1 [at depth  $z_1 - 2(n-p)H = z_1 - 2H$ ], and receiver 2. Hence, the difference between the free-space propagation path  $R_{s,2,n=1}^-$  (dash-dotted line) and  $R_{s,1,p=0}^-$  (dashed line) is equal to the free-space distance  $R_{1,2,n-p=1}^-$  (dotted line), i.e., the distance between the image of receiver 1 and receiver 2 itself.

$$\Delta_{1,2}^{\sigma,\zeta} = \nu Q^2 \int_{\omega_1}^{\omega_2} \frac{d\omega}{\pi} \int_{-\infty}^{+\infty} d\mathbf{r}_s \sum_{p=-\infty}^{p=+\infty} \sum_{n=-\infty}^{n=+\infty} (-1)^{|p|+|n|} V_b^{|p|+|n|} \times \left( \frac{e^{i\omega(\tau + (R_{s,1,p}^\sigma - R_{s,2,n}^\zeta)/c_0)} \cdot e^{-\omega(R_{s,1,p}^\sigma + R_{s,2,n}^\zeta)c_i/c_0^2}}{R_{s,1,p}^\sigma R_{s,2,n}^\zeta} \right), \quad (8)$$

where the sign exponents symbols are [using the notation of Eq. (2)]  $\sigma = \pm$  and  $\zeta = \pm$ . The double sum over image index  $p$  and  $n$  is associated with the particular images of the noise sources recorded by receiver 1 and receiver 2, respectively. The arrival times of the NCF,  $\tau$ , are thus set by the difference of travel times  $R_{s,1,p}^\sigma/c_0$  (from the noise source image of order  $p$  to receiver 1) and  $R_{s,2,n}^\zeta/c_0$  (from the noise source image of order  $n$  to receiver 2). On the other hand, the volume attenuation for the amplitude associated with these arrival times depends on the sum of those travel times  $-\omega(R_{s,1,p}^\sigma + R_{s,2,n}^\zeta)c_i/c_0^2$  and on the accumulated amplitude damping due to bottom reflection,  $V_b^{|p|+|n|}$ . Thus, the contributions to the NCF of distant noise sources as well as the contributions resulting from high-order images (which follow steep propagation paths) will be attenuated quicker.

The last step in the image formulation of the NCF involves performing the horizontal spatial integration over the whole distribution of noise sources. Section II C presents the mathematical derivations for the first term only,  $\Delta_{1,2}^{-,-}$  (i.e.,  $\sigma = \zeta = -$ ), of the NCF [see Eq. (7)]. The values of the three other terms can be directly computed by simple substitution, in Eq. (8), of a different pair  $(R_{s,1,p}^\sigma, R_{s,2,n}^\zeta)$ , for  $\sigma = \pm$  and  $\zeta = \pm$ .

## C. Evaluation of the spatial integration of the NCF

### 1. The stationary phase approximation

In the high-frequency regime, the spatial integration in Eq. (8) over the distribution of noise sources can be estimated using a stationary phase approximation<sup>20</sup> where the phase  $\Phi_{1,2}^-(\mathbf{r}_s)$  [associated with term  $\Delta_{1,2}^-$ ; see Eq. (8)] corresponds to

$$\Phi_{1,2}^-(\mathbf{r}_s) = \omega(\tau + (R_{s,1,p}^- - R_{s,2,n}^-)/c_0). \quad (9)$$

For this method, the spatial integration can be estimated by first finding the noise source locations where  $\Phi_{1,2}^-(\mathbf{r}_s)$  has

vanishing derivatives [i.e., the extrema of  $\Phi_{1,2}^-(\mathbf{r}_s)$ ], then evaluating the spatial integral in the vicinity of each of these locations by using a Taylor series expansion, and finally summing these contributions.

The particular noise source locations  $[\tilde{\mathbf{r}}_s = (\tilde{x}_s, \tilde{y}_s)]$  corresponding to the extrema of the phase function  $\Phi_{1,2}^-(\tilde{\mathbf{r}}_s)$  are determined by the two spatial conditions, for a given pair of indices  $(n, p)$

$$\tilde{y}_s = 0, \quad (10)$$

$$\frac{\tilde{x}_s}{\tilde{x}_s^2 + (z_1 - z_s + 2pH)^2} = \frac{\tilde{x}_s - L}{(\tilde{x}_s - L)^2 + (z_2 - z_s + 2nH)^2}. \quad (11)$$

The first condition, in Eq. (10), implies that noise sources contributing to the NCF are located in the endfire direction, with respect to the two receivers. The second condition in Eq. (11) specifies a discrete set of noise sources located on the endfire line due to the boundary conditions at the interfaces of the waveguide. The remainder of this section will show that these noise sources create a time delay  $\tau$  in the NCF between receiver 1 and receiver 2 related to the arrival time of the TDGF [see Eq. (1)] between these two receivers.

### 2. Geometric interpretation of the arrival times of the NCF derived from the stationary phase conditions

Figure 2 gives a geometric interpretation of the arrival times of the NCF derived from the stationary phase conditions [see Eq. (10) and Eq. (11)], for a given pair of image indices  $(n, p)$ . The distance between the noise source and receiver 1 can be expressed as  $R_{s,1,p}^- = \sqrt{[\tilde{x}_s^b]^2 + ((z_1 + 2(p-n)H) - (z_s - 2nH))^2}$ . Hence,  $R_{s,1,p}^-$  is also the distance between the  $(-n)$ th image of the noise source and the  $(p-n)$ th image of receiver 1. Consider the noise source located at  $\tilde{\mathbf{r}}_s^b = (\tilde{x}_s^b, \tilde{y}_s^b = 0)$ , such that the  $(-n)$ th image of this noise source, the  $(p-n)$ th image of receiver 1, and receiver 2 itself are all aligned. The resulting arrival time  $\tau_G^-$  of the NCF is then

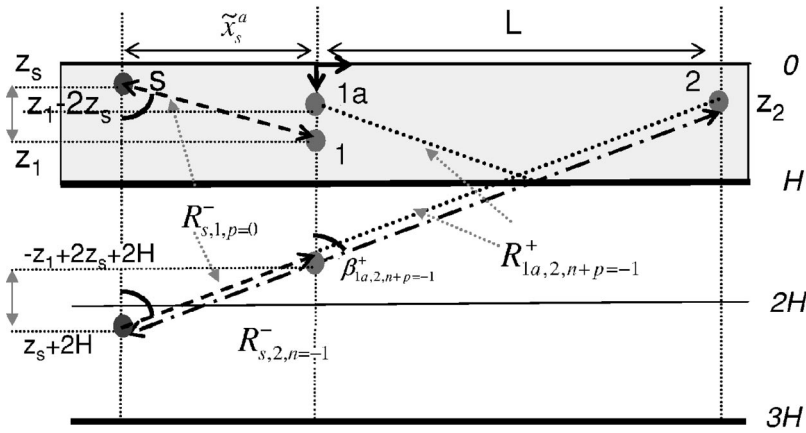


FIG. 3. Geometric construction of the location of the noise source corresponding to the second solution of the stationary phase conditions  $\tilde{\mathbf{r}}_s^a = (\tilde{x}_s^a, \tilde{y}_s^a = 0)$ , for  $n = -1$  and  $p = 0$  [see Eq. (14) and Eq. (15)]. The noise source image orders considered are  $n = -1$  and  $p = 0$ . Note the alignment between the noise source image [at depth  $z_s - 2(n-p)H = z_s + 2H$ ], the image of receiver 1 [at depth  $-(z_1 - 2z_s + 2(n+p)H) = -z_1 + 2z_s + 2H$ ], and receiver 2. Hence, the difference between the free-space propagation paths  $R_{s,1,p=0}^-$  (dash-dotted line) and  $R_{s,2,n=-1}^-$  (dashed line) is equal to the free-space distance  $R_{1a,2,n+p=-1}^+$  (dotted line), i.e., the distance between the image located at a depth  $-(z_1 - 2z_s + 2(n+p)H)$  and receiver 2 itself.

$$\tau_{G^-}^- = \frac{R_{s,2,n}^- - R_{s,1,p}^-}{c_0} = \pm \frac{R_{1,2,n-p}^-}{c_0} = \pm \frac{\sqrt{L^2 + (z_2 - z_1 + 2(n-p)H)^2}}{c_0}. \quad (12)$$

Hence,  $\tau_{G^-}^-$  is also the arrival time of the TDGF between the  $(p-n)$ th image of receiver 1 and receiver 2. Using this geometric construction, a closed-form expression for the noise source location  $\tilde{\mathbf{r}}_s^b = (\tilde{x}_s^b, \tilde{y}_s^b)$  is then

$$\tilde{x}_s^b = -\text{sign}(\tau)(z_1 - z_s + 2pH) \cdot \tan(\beta_{1,2,n-p}^-); \quad \tilde{y}_s^b = 0, \quad (13)$$

$$\tan(\beta_{1,2,n-p}^-) = \frac{L}{z_2 - z_1 + 2(n-p)H},$$

where  $\beta_{1,2,n-p}^-$  is the angle made by the line joining the  $(-n)$ th image of this noise source, the  $(p-n)$ th image of receiver 1, and receiver 2 with respect to the vertical axis (see Fig. 2). Furthermore, the corresponding phase  $\Phi_{1,2}^- (\tilde{\mathbf{r}}_s^b)$  [see Eq. (9)] reduces to  $\Phi_{1,2}^- (\tilde{\mathbf{r}}_s^b) = \omega(\tau \pm \tau_{G^-}^-)$ , which is independent of the noise source location  $\tilde{\mathbf{r}}_s^b$ . This geometric condition on the noise source location gives an interpretation of the stationary phase conditions expressed by Eq. (10) and Eq. (11).

Similarly, Fig. 3 shows a geometric construction for a second noise source location  $\tilde{\mathbf{r}}_s^a = (\tilde{x}_s^a, \tilde{y}_s^a = 0)$  which satisfies the same stationary phase conditions for the pair of image indices  $(n, p)$ . Another way to express the distance between the noise source and receiver 1 is  $R_{s,1,p}^- = \sqrt{|\tilde{\mathbf{r}}_s^a|^2 + ((-z_1 + 2z_s - 2(p+n)H) - (z_s - 2nH))^2}$ . Introduce an extra receiver 1a located at  $(x_1 = 0, y_1 = 0, z_1 - 2z_s)$ , which is shifted in depth by a distance  $-2z_s$  with respect to receiver 1. In this case,  $R_{s,1,p}^-$  corresponds the distance between the  $(-n)$ th image of the noise source and the  $(p+n)$ th image of receiver 1a. If we now consider the noise source located at  $\tilde{\mathbf{r}}_s^a$ , so that the  $(-n)$ th image of this noise source, the  $(p+n)$ th image of receiver 1a, and receiver 2 itself are all aligned, the resulting arrival time  $\tau_{s^-}^-$  of the NCF is then

$$\tau_{s^-}^- = \frac{R_{s,2,n}^- - R_{s,1,p}^-}{c_0} = \pm \frac{R_{1a,2,n+p}^+}{c_0} = \pm \frac{\sqrt{L^2 + (z_2 + (z_1 - 2z_s) + 2(n-p)H)^2}}{c_0}. \quad (14)$$

Hence,  $\tau_{s^-}^-$  is also the arrival time of the TDGF between the  $(p+n)$ th image of receiver 1a (located at a shifted depth  $z_1 - 2z_s$ ) and receiver 2. Note that  $\tau_{s^-}^-$  now depends on the value of the noise source depth  $z_s$ . Using this geometric construction, a closed-form expression for the noise source location  $\tilde{\mathbf{r}}_s^a = (\tilde{x}_s^a, \tilde{y}_s^a)$  is

$$\tilde{x}_s^a = -\text{sign}(\tau)(z_1 - z_s + 2pH) \cdot \tan(\beta_{1a,2,n+p}^+); \quad \tilde{y}_s^a = 0, \quad (15)$$

$$\tan(\beta_{1a,2,n+p}^+) = \frac{L}{z_2 + (z_1 - 2z_s) + 2(n+p)H},$$

where  $\beta_{1a,2,n+p}^+$  is the angle made by the line joining the  $(-n)$ th image of this noise source, the  $(p+n)$ th image of receiver 1a, and receiver 2 with respect to the vertical axis (see Fig. 3). The stationary phase condition now yields  $\Phi_{1,2}^- (\tilde{\mathbf{r}}_s^a) = \omega(\tau \pm \tau_{s^-}^-)$ , which is independent of the horizontal coordinates of the noise source  $(\tilde{x}_s^a, \tilde{y}_s^a)$ .

Thus, the noise sources located at  $(\tilde{\mathbf{r}}_s^b)$  and  $(\tilde{\mathbf{r}}_s^a)$ , satisfy the stationary phase conditions for  $\Phi_{1,2}^-$  [see Eq. (10) and Eq. (11)] and are in the endfire direction with respect to the

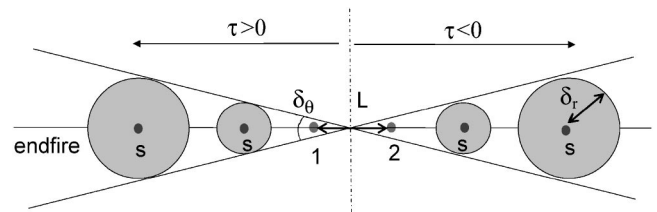


FIG. 4. Top view of the ocean surface. The noise sources making a significant contribution to the image of receiver 1 of order  $n \pm p$  in  $C_{1,2}(\tau)$  are located within a disk of radius  $\delta_r$  [see Eq. (17)] from the noise source locations (s) determined by the stationary phase conditions [see Eqs. (10), (11)], which are on the endfire direction.  $\delta_\theta$  is the aperture of the cone in which all of the noise sources contributing to the image of receiver 1 of order  $n \pm p$  lie. By definition of the cross-correlation function  $C_{1,2}(\tau)$  [see Eq. (5)], the noise sources associated with positive arrival times are located at a range  $x_s < 0$ , while the noise sources associated with negative arrival times are located at a range  $x_s > L$ .

two receivers. These noise sources contribute to two specific arrival times of the NCF: (1)  $\pm \tau_G^-$ , which is also an arrival time of the TDGF between receiver 1 and 2; and (2)  $\pm \tau_s^-$ , which is also an arrival time of the TDGF between receiver 1a and 2 and depends on the noise source depth  $z_s$ . The sign of these arrival times depends on the relative depth position of the noise source and the two receivers (see the Appendix for a complete discussion). Positive arrival times  $\tau$  correspond to the correlation of noise sources having a range  $x_s < 0$  (i.e., being on the left of receiver 1 in the endfire direction). On the other hand, negative arrival times  $\tau$  result from the correlation of noise sources having a range  $x_s > L$  (i.e., being on the right of receiver 2, in the endfire direction) (see Fig. 4). Since the noise sources are distributed symmetrically around the two receivers' locations, the NCF,  $C_{1,2}(\tau)$ , for  $\tau > 0$  will be a mirror image of the NCF,  $C_{1,2}(\tau)$ , for  $\tau < 0$ , with respect to the time origin  $\tau = 0$ .

### 3. Spatial resolution of the NCF

Since the phase  $\Phi_{1,2}^-(\mathbf{r}_s)$ , has vanishing derivatives in the vicinity of noise source location  $\mathbf{r}_s^b$ , it can be expressed as a second-order Taylor series (and similarly for  $\mathbf{r}_s^a$ )

$$\Phi_{1,2}^-(\mathbf{r}_s) = \Phi_{1,2}^-(\tilde{\mathbf{r}}_s^b) + \frac{1}{2}(\mathbf{r}_s - \tilde{\mathbf{r}}_s^b) \cdot [(\mathbf{r}_s - \tilde{\mathbf{r}}_s^b) \cdot \nabla_{\mathbf{r}_s}(\nabla_{\mathbf{r}_s} \Phi_{1,2}^-(\mathbf{r}_s))]_{\mathbf{r}_s = \tilde{\mathbf{r}}_s^b}. \quad (16)$$

Equation (16) can be used to evaluate the spatial integration for the partial cross correlation between the two receivers  $\Delta_{1,2}^-(\tau)$  [see Eq. (8)] using the stationary phase approximation. Additionally, Eq. (16) shows that the spatial area, centered on the noise source location,  $\tilde{\mathbf{r}}_s^b$  or  $(\mathbf{r}_s^a)$  (in the horizontal plane of the noise sources), which makes a significant contribution to  $\Delta_{1,2}^-(\tau)$  is of the order of  $[\nabla_{\mathbf{r}_s}(\nabla_{\mathbf{r}_s} \Phi_{1,2}^-(\mathbf{r}_s))]^{-1}$ , for  $\mathbf{r}_s = \mathbf{r}_s^a$  or  $\mathbf{r}_s^b$ . This quantity corresponds to a disk area centered on the noise source location  $\tilde{\mathbf{r}}_s^b$  of radius  $\delta_r$  (see Fig. 4)

$$\delta_r = |\tilde{x}_s^b| \cdot \delta_\theta, \quad \delta_\theta = \left( \frac{\sqrt{\omega R_{1,2,n-p}^- \sin(\beta_{1,2,n-p}^-)}}{c_0} \right)^{-1} \cdot \sqrt{\frac{|\tilde{x}_s^b - L|}{|\tilde{x}_s^b|}}, \quad (17)$$

where  $\delta_\theta$  is the aperture of the cone in which the noise sources associated with the arrival times  $\tau_G^-$  or  $\tau_s^-$  of the NCF lie [see Eq. (12) and Eq. (14)]. When using a coordinate system centered on the location  $(L/2, 0, 0)$  (i.e., at equal range from receiver 1 and receiver 2) instead of receiver 1, the new range coordinate for the source location  $\tilde{\mathbf{r}}_s^b$  is then shifted to  $|\tilde{x}_s^b - L/2|$  and this coordinate system is symmetrical (with respect to the two receivers)  $|\tilde{x}_s^b| = |\tilde{x}_s^b - L|$ . Similar results can be derived for the location  $\mathbf{r}_s^a$ . Thus, in this symmetrical coordinate system, the expression of the angular aperture  $\delta_\theta$  is then simply inversely proportional to

$$\frac{\sqrt{\omega R_{1,2,n-p}^- \sin(\beta_{1,2,n-p}^-)/c_0}}{\sqrt{\omega R_{1a,2,n+p}^+ \sin(\beta_{1a,2,n+p}^+)/c_0}}.$$

The angular aperture  $\delta_\theta$  determines the amount of noise sources contributing to the arrival times  $\tau_G^-$  or  $\tau_s^-$  of the NCF. The parameter  $\delta_\theta$  decreases with the image order  $n \pm p$  for the noise source images considered due to the factor  $\sin(\beta_{1,2,n-p}^-)$  [or  $\sin(\beta_{1a,2,n+p}^+)$ ], and is inversely proportional to the product of the wave number  $(\omega/c_0)$  times the free-space distance  $R_{1,2,n-p}^-$  (or  $R_{1a,2,n+p}^+$ ). The parameter  $\delta_\theta$  can be interpreted as a directivity pattern of the NCF, which acts as a beamforming process on the endfire direction for the homogeneous horizontal noise source distributions. Equation (17) then appears as a generalization of previous free-space results<sup>6</sup> to the case of an oceanic waveguide, and includes now the dependency on the image order  $n \pm p$  and waveguide geometry.

### 4. Final formulation of the NCF and its time derivative

Using the results of Secs. II C 1 and II C 2 and noting that  $d(e^{i\omega\tau})/d\tau = i\omega e^{i\omega\tau}$ , the derivative of the partial cross correlation between the two receivers  $\Delta_{1,2}^-(\tau)$ , [see Eq. (2) and Eq. (8)] can then be simplified to

$$\frac{d\Delta_{1,2}^-}{d\tau} = \nu Q^2 c_0 \int_{\omega_1}^{\omega_2} d\omega \sum_{p=-\infty}^{p=+\infty} \sum_{n=-\infty}^{n=+\infty} (-1)^{|p|+|n|} V_b^{|p|+|n|} \left( \frac{e^{i\omega(\tau \pm R_{1,2,n-p}^-/c_0)} \cdot e^{-\omega(|\tilde{x}_s^b| + |\tilde{x}_s^b - L|)/\sin(\beta_{1,2,n-p}^-) \cdot c_i/c_0^2}}{R_{1,2,n-p}^-} + \frac{e^{i\omega(\tau \pm R_{1a,2,n+p}^+/c_0)} \cdot e^{-\omega(|\tilde{x}_s^a| + |\tilde{x}_s^a - L|)/\sin(\beta_{1a,2,n+p}^+) \cdot c_i/c_0^2}}{R_{1a,2,n+p}^+} \right). \quad (18)$$

In this geometry, the  $(-p)$ th and  $(-n)$ th images of this noise source will contribute to a pair of arrival times of the NCF, determined by the stationary phase conditions [see Eq. (12) and Eq. (14)]:  $\tau_G^- = \pm R_{1,2,n-p}^-/c_0$  ( $\tau_s^- = \pm R_{1a,2,n+p}^+/c_0$ ) for the temporal derivative of the NCF  $d\Delta_{1,2}^-/d\tau$ . The arrival time  $\tau_s^-$  depends on the noise

source depth  $z_s$  and is close to the arrival times of the TDGF between receiver 1 and 2 since  $R_{1a,2,n+p}^+/c_0 \approx R_{1,2,n+p}^+/c_0$  when  $z_s$  is small (i.e.,  $z_1 - 2z_s \approx z_1$ ). Similar relationships between the time-arrival structure of the time derivative of the NCF and the TDGF have also been derived for ultrasonic cavities.<sup>1,2</sup>

The three other cross terms  $\Delta_{1,2}^{\sigma,\zeta}$ , for  $\sigma=\pm$  and  $\zeta=\pm$ -as defined by Eq. (8), of the NCF  $C_{1,2}(\tau)$  [see Eq. (5)], can be computed in a similar way to the previous derivation for  $\Delta_{1,2}^{\pm,\pm}(\tau)$ . Based on the same stationary phase arguments, each time derivative of these cross terms yields a pair of arrival times  $(\tau_G^{\pm,\pm}, \tau_s^{\pm,\pm})$ . Figure 5 illustrates the resulting arrival-time structure of the NCF for a given value of the image order  $n \pm p$ . Thus, it appears that some of the arrival times of the NCF exactly match the arrival times of the TDGF between receiver 1 and 2:  $\tau_G = \sqrt{L^2 + (z_2 \pm z_1 + 2(n \pm p)H)^2}/c_0$  [note that the exponent  $(\cdot)^{\pm}$  has been dropped since we are discussing now the complete arrival-time structure of the NCF  $C_{1,2}(\tau)$  and no longer  $\Delta_{1,2}^{\pm,\pm}$  alone]. But, additional times delays also exist, whose values depend on the noise source depth  $z_s$ :  $\tau_s = \sqrt{L^2 + (z_2 \pm z_1 \pm 2z_s + 2(n \pm p)H)^2}/c_0$  [see Eq. (14)]. The amplitudes corresponding to the arrival times  $\tau_G$  and  $\tau_s$  have opposite phase [see Eq. (7)].

Similar results can be derived based on earlier modal formulations of the NCF (Ref. 13) for the case of the Pekeris waveguide: the dependency on the noise source depth  $z_s$  ap-

pears explicitly in the arrival times by transforming the modal sum into a infinite sum of images.<sup>31</sup> Furthermore, similar dependency on the noise source depth [through the term  $\pm 2z_s$ ; see Eq. (19)] for the vertical coherence of sea-surface ambient noise has been previously reported.<sup>26</sup> The expression depends on various combinations depth differences  $z_2 \pm z_1$  and  $z_2 \pm z_1 \pm 2z_s$ .

#### D. Simplified image formulation of the NCF

This section simplifies this result for the case of (1) no volume attenuation; or (2) a small source depth  $z_s$  (dipole expansion). A direct interpretation of the arrival-time structure of the derivative of the time-averaged NCF then becomes apparent.

##### 1. Case of no volume attenuation

In the limit of no volume attenuation ( $c_i=0$ ), the expression for the time derivative of the NCF  $dC_{1,2}(\tau)/d\tau$  [see Eq. (7) and Eq. (18)] can be expressed simply as, using the notation of Eq. (1) and Eq. (2)

$$\begin{aligned} \frac{dC_{1,2}(\tau)}{d\tau} = & \nu Q^2 c_0 \int_{\omega_1}^{\omega_2} d\omega \sum_{p=-\infty}^{p=+\infty} \sum_{n=-\infty}^{n=+\infty} (-1)^{|p|+|n|} V_b^{|p|+|n|} [2(G_{n-p}^-(\mathbf{r}_2, z_2, \mathbf{r}_1, z_1; \tau) - G_{n+p}^+(\mathbf{r}_2, z_2, \mathbf{r}_1, z_1; \tau)) \\ & - (G_{n-p}^-(\mathbf{r}_2, z_2, \mathbf{r}_1, z_1 - 2z_s; \tau) - G_{n+p}^+(\mathbf{r}_2, z_2, \mathbf{r}_1, z_1 - 2z_s; \tau)) - (G_{n-p}^-(\mathbf{r}_2, z_2, \mathbf{r}_1, z_1 + 2z_s; \tau) \\ & - G_{n+p}^+(\mathbf{r}_2, z_2, \mathbf{r}_1, z_1 + 2z_s; \tau))], \end{aligned} \quad (19)$$

where

$$\begin{aligned} G_l^-(\mathbf{r}_2, z_2, \mathbf{r}_1, z_1; t) &= \frac{e^{i\omega(t - R_{1,2,l}^-/c_0)}}{R_{1,2,l}^-}, \\ G_l^+(\mathbf{r}_2, z_2, \mathbf{r}_1, z_1; t) &= \frac{e^{i\omega(t - R_{1,2,l}^+/c_0)}}{R_{1,2,l}^+}. \end{aligned} \quad (20)$$

The derivative of the NCF  $dC_{1,2}(\tau)/d\tau$  [see Eq. (19)] can then be related to three TDGF: (1)  $G_{n \pm p}^{\pm}(\mathbf{r}_2, z_2, \mathbf{r}_1, z_1; \tau)$ , the TDGF between receiver 2 and receiver 1 itself which has double amplitude; (2)  $G_{n \pm p}^{\pm}(\mathbf{r}_2, z_2, \mathbf{r}_1, z_1 - 2z_s; \tau)$ , the TDGF between receiver 2

and a receiver (referred to as receiver 1a in Sec. II C 2) at a location  $(\mathbf{r}_1, z_1 - 2z_s)$  shifted in depth with respect to receiver 1; and (3)  $G_{n \pm p}^{\pm}(\mathbf{r}_2, z_2, \mathbf{r}_1, z_1 + 2z_s; \tau)$ , the TDGF between receiver 2 and a receiver at a location  $(\mathbf{r}_1, z_1 + 2z_s)$  also shifted in depth with respect to receiver 1.

##### 2. Dipole expansion

When the noise source depth  $z_s$  is very small compared to the depth of the two receivers, the source and its surface-reflected image (at a depth  $-z_s$ ) acts as a dipole. The dipole radiation pattern can be derived from the last expression of the noise cross correlation [see Eq. (19)] using second-order expansion in terms of  $z_s$

$$\begin{aligned} \frac{dC_{1,2}^{\text{Dipole}}(\tau)}{d\tau} = & 2z_s^2 \nu Q^2 c_0 \int_{\omega_1}^{\omega_2} \frac{d\omega}{2\pi} \sum_{p=-\infty}^{p=+\infty} \sum_{n=-\infty}^{n=+\infty} (-1)^{|p|+|n|} V_b^{|p|+|n|} \frac{\omega}{c_0} \left( \frac{e^{i\omega(\tau \pm R_{1,2,n-p}^-/c_0)} \cdot e^{-\omega(|x_s^p| + |\tilde{x}_s^p - L|)/\sin(\beta_{1,2,n-p}^-) \cdot c_i/c_0^2}}{R_{1,2,n-p}^-} \right. \\ & \left. \times \cos^2(\beta_{1,2,n-p}^-) - \frac{e^{i\omega(\tau \pm R_{1,2,n+p}^+/c_0)} \cdot e^{-\omega(|x_s^a| + |\tilde{x}_s^a - L|)/\sin(\beta_{1,2,n+p}^+) \cdot c_i/c_0^2}}{R_{1,2,n+p}^+} \cos^2(\beta_{1,2,n+p}^+) \right), \end{aligned} \quad (21)$$

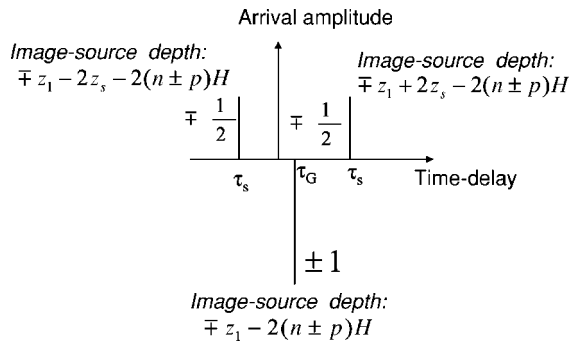


FIG. 5. Schematic of the structure of the time-delay arrivals of the noise cross correlation  $C_{1,2}(\tau)$  for a given value of the image indices  $n \pm p$ . The three correlation arrival times can be related to the superimposed arrival-time structure of three TDGFs between sources located at (1) a depth  $z_1$  (i.e., receiver 1, corresponding to a TDGF arrival  $\tau_G$ ) or (2)  $z_1 \pm 2z_s$  (i.e., two distinct locations shifted in depth from the location of receiver 1, corresponding to a TDGF arrival  $\tau_s$ ) and a receiver located at depth  $z_2$  (receiver 2). The depth of the images of the three equivalent sources are indicated above each of the three corresponding arrival times of the NCF. The amplitudes associated with the two arrival times  $\tau_s$  are equal and are half the amplitude associated with the time delay  $\tau_G$  as well as having opposite sign. Thus, for  $z_s \rightarrow 0$ , these three arrival times merge and yield a dipole radiation pattern.

where the expressions of  $\beta_{1a,2,n+p}^+ = \beta_{1,2,n+p}^+$  and  $R_{1a,2,n+p}^+ = R_{1,2,n+p}^+$  were evaluated for  $z_s = 0$ . The three arrival times of the NCF represented in Fig. 5 merge for  $z_s \rightarrow 0$ , thus creating a dipole effect. The associated dipole radiation pattern [represented by the factors  $\cos^2(\beta_{1,2,n \pm p}^{\pm p})$  in Eq. (21)] yields a stronger amplitudes for the arrival times of the NCF associated with a high image order ( $n \pm p$ ).

The following section discusses the influence of the source depth  $z_s$  and the effective receiver bandwidth ( $[\omega_1, \omega_2]$ ) on the cross-arrival times of the NCF which can be effectively measured.

### E. Influence of the noise source depths and the receiver's frequency bandwidth

The previous sections showed how the distribution of the various arrival times measured by the time derivative of the NCF  $C_{1,2}(\tau)$  depends, among others factors, on the noise source depth  $z_s$  [see Fig. 5, Eq. (18), and Eq. (19)]. In practice, the determination of the depth  $z_s$  of the acoustically active bubbles from a breaking event is a complex problem (since it may depend on the bubble size, density, or acoustic frequency of interest) and is an ongoing research topic.<sup>24,25</sup> For instance, this depth was estimated to be 1.5 m, based on inversion of wave-breaking sound measured at wind speed of 10 m/s or greater in the sea-surface bubble layer.<sup>26</sup>

Only the arrival times,  $\tau_s = \sqrt{L^2 + (z_2 \pm z_1 \pm 2z_s + 2(n \pm p)H)^2} / c_0$  of the time derivative of the cross correlation  $dC_{1,2}(\tau)/d\tau$ , that do not exactly match the arrival times of the TDGF [see Eq. (1)], depend on the spatial distribution of  $z_s$  (i.e., the depth dependency of the acoustically active noise bubbles). Note that the notation  $\tau_s$  represent both depth shifts  $\pm 2z_s$ . On the other hand, the arrival times  $\tau_G = \sqrt{L^2 + (z_2 \pm z_1 + 2(n \pm p)H)^2} / c_0$  of  $dC_{1,2}(\tau)/d\tau$  that are independent of the value  $z_s$  for each noise source considered correspond exactly to an arrival time of the TDGF. Thus, for a given value of the image order  $n$

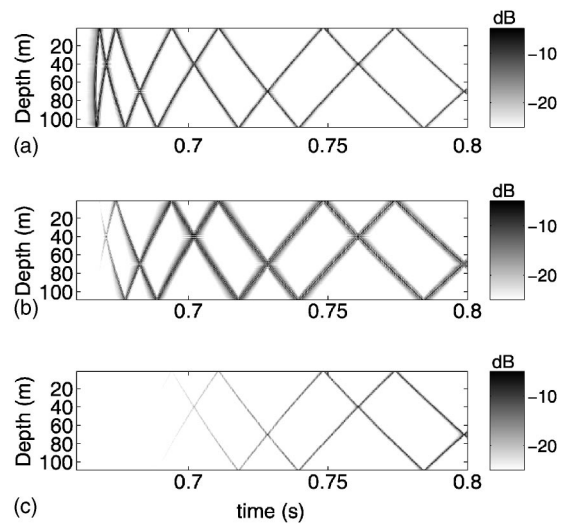


FIG. 6. Positive time-delay wavefronts of  $C_{1,2}(\tau)$ , for varying depth of receiver 2 in the water column, in the case of a simple oceanic waveguide ( $H = 110$  m,  $L = 1$  km,  $z_1 = 70$  m) for both  $z_s = 1$  m and  $z_s = 0.1$  m [(b) and (c)]. It also provides a comparison with the TDGF of this waveguide [(a)]. The bandwidth is  $[\omega_1 = 1$  kHz,  $\omega_2 = 3$  kHz].

$\pm p$  (i.e., a given set of noise sources), the arrival times  $\tau_s$  should be spread around the constant time delay  $\tau_G$  if the variations of  $z_s$  are large. Furthermore, the amplitudes of the signals occurring at these arrival times  $\tau_s$  should be much weaker than the amplitude of the signals occurring at the arrival times  $\tau_G$  since these last ones result from the coherent sum of all the random noise source amplitudes. Consequently, if the random noise sources  $z_s$  are widely distributed in the water column, the high signal amplitude of the temporal derivative of the NCF  $dC_{1,2}(\tau)/d\tau$  should occur at arrival times  $\tau_G$  and thus the temporal derivative of the NCF would better match the structure of the TDGF. A similar effect was also predicted by an earlier study of the cross correlation between a pair of receivers, in the presence of a set of controlled sound sources located across the water column depth.<sup>9</sup>

For a given value of the noise source depth  $z_s$  and of the image indices  $n \pm p$ , the ability to discriminate between the arrival times  $\tau_s$  and  $\tau_G$  is set by the temporal resolution  $\Delta T$  of the cross-correlation process [i.e., here the inverse of the frequency bandwidth  $\Delta T = 2\pi / (\omega_2 - \omega_1)$ ]. For sufficiently large bandwidth, i.e., if  $\Delta T < |\tau_G - \tau_s|$ , the arrival-time structure of  $dC_{1,2}(\tau)/d\tau$  can be resolved. Figure 6 shows wavefronts of  $dC_{1,2}(\tau)/d\tau$ , occurring at positive arrival times, for varying depth of receiver 2 in the water column, in the case of a simple oceanic waveguide ( $H = 110$  m,  $L = 1$  km,  $z_1 = 70$  m) for both  $z_s = 1$  m and  $z_s = 0.1$  m [Figs. 6(b) and (c)]. It also provides a comparison with the TDGF of this waveguide [Fig. 6(a)]. Here, the frequency bandwidth is from 1 to 3 kHz; thus,  $\Delta T \approx 0.5$  ms. For  $|n \pm p| > 2$  and  $z_s = 1$  m, the various wavefronts for  $dC_{1,2}(\tau)/d\tau$  can be resolved. They are thickened compared to the wavefronts of the TDGF since they correspond to the merging of three different arrival times  $\tau_G$  and  $\tau_s$  [compare Figs. 6(a) and (b)].

In the opposite case, if  $\Delta T > |\tau_G - \tau_s|$ , the temporal resolution is then too coarse and does not allow separation of

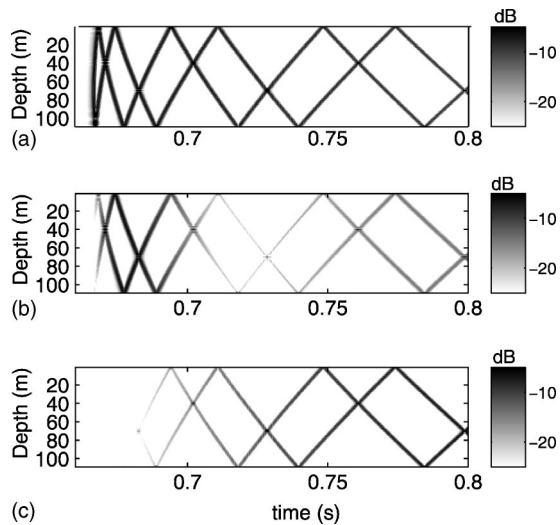


FIG. 7. Same parameters as Fig. 6 but using a previous normal-mode formulation (Ref. 13). Note the similarity of the arrival-time structure obtained with the ray formulations in Fig. 6.

the signals occurring at these time delays  $\tau_G$  and  $\tau_s$ . Furthermore, the signals occurring at arrival times  $\tau_s$  average down with the signals occurring at  $\tau_G$  since they are of opposite phase [see Eq. (19)]. In practice, the separation between  $\tau_G$  and  $\tau_s$  decreases with decreasing image order  $n \pm p$ . Thus, the amplitudes of the signals occurring at early arrival times  $\tau_G$  should then be weaker compared to subsequent arrivals. This corresponds to a dipole effect as predicted by the asymptotic formulas for small values of  $z_s$  in Eq. (21) [see Fig. 6(c), for  $z_s = 0.1$  m].

Figure 7 displays the wavefront structure of the TDGF and the noise cross correlation  $dC_{1,2}(\tau)/d\tau$  using a previous normal-mode formulation,<sup>13</sup> for the same parameters as in Fig. 6. The good agreement between Fig. 6 and Fig. 7 confirms the equivalence between the ray formulation described in this article and previous normal-mode formulations. The temporal structure is identical but the discrepancies in amplitude are due to (1) the difference in modeling volume and bottom attenuation; and (2) the use of a finite number of images as well as a finite number of modes.

### III. PRACTICAL CONSIDERATIONS FOR SEA EXPERIMENTS

The successful implementation of the ambient noise cross-correlations process to extract coherent wavefronts will be mainly determined by three factors: (1) hardware configuration (see below); (2) the choice of the duration of the ambient noise recordings used for the correlation process; and (3) the spatio-temporal distribution of the ambient noise sources in the environment surrounding the receivers. The following discussion suggests optimal conditions for these three factors.

First, the noise cross-correlation process requires the use of time-synchronized receivers and the absence of relative motions between them, in order to precisely determine the correlation arrival times. Moored or bottom-mounted arrays, having a common time clock for each of the array elements recordings, should provide an efficient hardware configura-

tion. Additionally, transducers having a flat frequency response over a large bandwidth would allow one to finely separate the various arrival times present in the noise cross correlations, even for noise source depths located relatively close to the sea surface (see Sec. II E).

Second, the choice of the recording time ( $T_{rec}$ , which determines the length of the cross-correlations window) is driven by the need to record a sufficient number of uncorrelated noise events in order to extract all the different paths of the TDGF from the noise cross-correlation process. Thus, the recording time  $T_{rec}$  should be larger than both (1) the dispersion time of the sound channel ( $T_{disp}$ , which corresponds to temporal spreading of the TDGF between the two receivers and which is also referred to as the break time of the system<sup>1</sup>); and (2) the statistical time  $T_{stat}$ . Under the ergodic assumption, the noise events are considered as realizations of a wide sense stationary stochastic process for which corresponding time and ensemble averages of this process are equivalent. In this case,  $T_{stat}$  is then the averaging time required to converge towards a homogeneous distribution of spatially and temporally uncorrelated noise sources [see Eq. (6)]. Any two particular noise events may have significant peaks in their cross-correlation function due to sidelobes and other correlated parts of their waveforms. Thus,  $T_{stat}$  depends on the particular characteristics of the noise source process and is usually an unknown parameter, but may be estimated using previous knowledge of the environment. Finally, the formulation of the cross-correlation process, as defined by Eq. (5), is valid for a stationary environment. Thus,  $T_{rec}$  should be smaller than the fluctuation's time scale of the environment  $T_{fluc}$  (such as currents or tidal periods). Otherwise, an estimate of noise cross correlation can be derived by averaging over several small correlations windows (such that  $T_{rec} < T_{fluc}$  for each correlation window). However, in the case of sea-surface motion and long averaging time, it is likely that  $T_{rec} > T_{fluc}$ . But, the main effect of sea-surface motion should only be to prevent the emergence of acoustic paths associated with sea-surface reflections in the estimate of the time-domain Green's function extracted from the noise cross-correlation function due to the destructive interference occurring during the long-time averaging. Overall, the practical use of the noise cross-correlation process should be optimal for the following order of the various time scales of the problem:  $T_{disp} < T_{stat} < T_{rec} < T_{fluc}$ .

Third, a random homogeneous distribution, in space and time, of uncorrelated noise point sources was assumed when deriving an analytical expression of NCF in Sec. II [see Eq. (6)]. The effect of the noise source depth  $z_s$  distribution can be clearly identified and recognized from the measured cross correlation (see Sec. II C.). The approximation of the noise sources being uncorrelated should hold for sufficiently long averaging times. However, the noise distribution may not be homogeneous in time or in space. For instance, temporal inhomogeneous distribution may result from some loud (compared to the average ambient noise level) noise events occurring at certain random times (e.g., a ship passing by, or an accidental burst of sound). The effectiveness of temporal and frequency equalization to remove high-energy single events (which differ from the homogeneous noise level) from

the noise recordings (previous to performing the cross-correlations) needs to be assessed. Additionally, a spatial anisotropic noise source distribution may be detrimental if there is no, or only a few, noise source(s) close to endfire direction of the two receivers. Indeed, these noise sources contribute, on average, to the arrival times of the NCF related to the arrival times of TDGF between these two receivers [see Eq. (10) and Eq. (11)]. It might also be the case that the bottom is not flat and is not equally absorbing in all spatial direction in the vicinity of a field test, thus leading to a specific directionality of the noise field. Thus, a careful study of the spatio-temporal distribution of the noise sources, in the environment of interest, is critical for explaining the performance of the noise cross-correlation process. On the other hand, when the extraction of coherent wavefronts from the noise cross-correlation process is successful, one may then attempt to invert for the spatio-temporal distributions of these noise sources.

#### IV. SUMMARY AND CONCLUSIONS

We have demonstrated theoretically how the arrival-time structure of the time-domain Green's function (TDGF) between two points can be estimated by cross correlating the ambient noise recorded at these two points, based on a model of surface-generated noise in the ocean. The ambient noise cross-correlation function (NCF)  $C_{1,2}(\tau)$  obtained after time averaging is dominated by the correlations that contain noise sources whose acoustic waves pass through both receivers, thus allowing the extraction of coherent wavefronts and corresponding arrival times. For the case of a homogeneous noise distribution, the spatial locations of the noise sources (all located in the vicinity of the endfire direction of the two receivers) contributing to a given coherent arrival time of the time derivative of the NCF were determined. This result provides a physical explanation of the nonintuitive relationship between the NCF and the TDGF. In particular, the relation between the arrivals times of the TDGF and these coherent arrival times of the time derivative of the NCF were established given the parameters of the oceanic waveguide (water depth, bottom and volume attenuation), the receiver (horizontal and vertical) separations, the spatial and temporal noise statistics parameters (e.g., depths of the noise sources, noise events creation rate), and the frequency bandwidth of interest. This simple image formulation of the NCF also explains the amplitude shading of the individual extracted coherent wavefronts, as observed experimentally in the ocean.<sup>6</sup> Thus, these theoretical results should be applicable in practice for the case of simple, range-independent, shallow-water waveguides, and may provide an upper-bound estimate for the performance of this noise cross-correlation process in more complex oceanic environments and noise sources distribution.

Ambient noise cross correlations may provide a mean to characterize the oceanic environment and its fluctuations (via the relationship between the arrival-time structure of the NCF and the TDGF) with little signal processing involved. The results presented in this article should be useful for interpreting the outcome of the noise cross-correlation process for other types of ambient noise mechanisms (e.g., biological

noise, shipping noise). High-frequency experiments could be used to determine more specifically the relationships between the spatial and temporal noise statistics of the ambient noise field of interest and the emergence of these coherent wavefronts from the NCF (e.g., shading of these wavefronts with respect to the actual TDGF wavefronts, convergence time towards the TDGF). Those relationships could also be used to monitor the evolution of the noise sources in the environment.

#### ACKNOWLEDGMENT

The research was sponsored by the Ocean Acoustics Program of the Office of Naval Research.

#### APPENDIX: SIGN OF THE ARRIVAL TIMES OF THE NCF DETERMINED BY THE STATIONARY PHASE CONDITIONS

For the case of a Pekeris waveguide, a geometric construction of the noise source locations ( $\tilde{\mathbf{r}}_s^a$  and  $\tilde{\mathbf{r}}_s^b$ ) satisfying the stationary phase conditions Eq. (10) and Eq. (11) was described in Secs. II C 1 and II C 2. This Appendix specifies the exact sign of the corresponding arrival times  $\tau_G^{\pm,-}$   $= \pm R_{1,2,n-p}^-/c_0$  and  $\tau_s^{\pm,-} = \pm R_{1a,2,n+p}^+/c_0$  of the NCF. Their sign is a function of the relative position in depth of the noise source and the two receivers in order to satisfy Eq. (11). The stationary phase  $\Phi_{1,2}^{\pm,-}(\mathbf{r}_s)$  at the locations ( $\tilde{\mathbf{r}}_s^b$ ) or ( $\tilde{\mathbf{r}}_s^a$ ) is then

$$\begin{aligned} \Phi_{1,2}^{\pm,-}(\tilde{\mathbf{r}}_s^b) &= \omega(\tau - \text{sign}(z_2 - z_1 + 2(n-p)H) \\ &\quad \cdot R_{1,2,n-p}^-/c_0), \quad \text{for } (z_2 - z_s + 2nH) > 0 \\ &\quad \text{and } (z_1 - z_s + 2pH) > 0; \end{aligned} \quad (\text{A1})$$

$$\begin{aligned} \Phi_{1,2}^{\pm,-}(\tilde{\mathbf{r}}_s^b) &= \omega(\tau + \text{sign}(z_2 - z_1 + 2(n-p)H) \\ &\quad \cdot R_{1,2,n-p}^-/c_0), \quad \text{for } (z_2 - z_s + 2nH) < 0 \\ &\quad \text{and } (z_1 - z_s + 2pH) < 0; \end{aligned}$$

and

$$\begin{aligned} \Phi_{1,2}^{\pm,-}(\tilde{\mathbf{r}}_s^a) &= \omega(\tau + \text{sign}(z_2 + z_1 - 2z_s + 2(n+p)H) \\ &\quad \cdot R_{1a,2,n+p}^+/c_0), \quad \text{for } (z_2 - z_s + 2nH) < 0 \\ &\quad \text{and } (z_1 - z_s + 2pH) > 0; \end{aligned} \quad (\text{A2})$$

$$\begin{aligned} \Phi_{1,2}^{\pm,-}(\tilde{\mathbf{r}}_s^a) &= \omega(\tau - \text{sign}(z_2 + z_1 - 2z_s + 2(n+p)H) \\ &\quad \cdot R_{1a,2,n+p}^+/c_0), \quad \text{for } (z_2 - z_s + 2nH) > 0 \\ &\quad \text{and } (z_1 - z_s + 2pH) < 0. \end{aligned}$$

<sup>1</sup>O. I. Lobkis and R. L. Weaver, "On the emergence of the Green's function in the correlations of a diffuse field," *J. Acoust. Soc. Am.* **110**, 3011–3017 (2001).

<sup>2</sup>R. L. Weaver and O. I. Lobkis, "Elastic wave thermal fluctuations, ultrasonic waveforms by correlation of thermal phonons," *J. Acoust. Soc. Am.* **113**, 2611–2621 (2003).

<sup>3</sup>J. Rickett and J. Claerbout, "Passive seismic imaging applied to synthetic data," *SEP* **92**, 83–90 (1996).

<sup>4</sup>J. Rickett and J. Claerbout, "Acoustic daylight imaging via spectral fac-

- torization: Helioseismology and reservoir monitoring,” *The Leading Edge* **18**, 957–960 (1999).
- <sup>5</sup>N. M. Shapiro and M. Campillo, “Emergence of broadband Rayleigh waves from correlations of the ambient seismic noise,” *Geophys. Res. Lett.* **31**, L07614 (2004).
- <sup>6</sup>P. Roux, W. A. Kuperman, and the NPAL Group, “Extracting coherent wavefronts from acoustic ambient noise in the ocean,” *J. Acoust. Soc. Am.* **116**, 1995–2003 (2004).
- <sup>7</sup>A. Derode, E. Larose, M. Tanter, J. Rosny, A. Tourin, M. Campillo, and M. Fink, “Recovering the Green’s function from field-field correlations in an open scattering medium,” *J. Acoust. Soc. Am.* **113**, 2973–2976 (2003).
- <sup>8</sup>A. Derode, E. Larose, M. Campillo, and M. Fink, “How to estimate the Green’s function of a heterogeneous medium between two passive sensors,” *Appl. Phys. Lett.* **83**, 3054–3056 (2003).
- <sup>9</sup>M. Campillo and A. Paul, “Long-range correlations in the diffuse seismic coda,” *Science* **299**, 547–549 (2003).
- <sup>10</sup>P. Roux and M. Fink, “Green’s function estimation using secondary sources in a shallow water environment,” *J. Acoust. Soc. Am.* **113**, 1406–1416 (2003).
- <sup>11</sup>R. Snieder, “Extracting the Green’s function from the correlation of coda waves: A derivation based on stationary phase,” *Phys. Rev. E* **69**, 046610 (2004).
- <sup>12</sup>K. Wapenaar, J. Thorbecke, and D. Draganov, “Relations between reflection and transmission responses of three-dimensional inhomogeneous media,” *Geophys. J. Int.* **156**, 179–194 (2004).
- <sup>13</sup>W. A. Kuperman and F. Ingenito, “Spatial correlation of surface generated noise in a stratified ocean,” *J. Acoust. Soc. Am.* **67**, 1988–1996 (1980).
- <sup>14</sup>M. J. Buckingham, “Spatial coherence of wind-generated noise in a shallow ocean channel,” *J. Acoust. Soc. Am.* **70**, 1412–1420 (1981).
- <sup>15</sup>T. C. Yang and K. Yoo, “Modeling the environmental influence on the vertical directionality of ambient noise in shallow water,” *J. Acoust. Soc. Am.* **101**, 2541–2554 (1997).
- <sup>16</sup>G. M. Wenz, “Acoustic ambient noise in the ocean: Spectra and sources,” *J. Acoust. Soc. Am.* **34**, 1936–1956 (1962).
- <sup>17</sup>R. K. Andrew, B. M. Howe, J. M. Mercer, and M. Dzieciu, “Ocean ambient sound: Comparing the 1960s with the 1990s for a receiver off the California coast,” *ARLO* **3**, 65 (2002). In this article, Wenz results have been compared to more recent data.
- <sup>18</sup>R. J. Urick, *Ambient Noise in the Sea* (Peninsula, Los Altos, CA, 1986).
- <sup>19</sup>M. J. Buckingham, “A theoretical model of ambient noise in a low-loss shallow water channel,” *J. Acoust. Soc. Am.* **67**, 1186–1192 (1980).
- <sup>20</sup>F. B. Jensen, W. A. Kuperman, M. B. Porter, and H. Schmidt, *Computational Ocean Acoustics* (American Institute of Physics, Woodbury, NY, 1994), pp. 33–34, 100–101, 183.
- <sup>21</sup>C. H. Harrison, “Formulas for ambient noise level and coherence,” *J. Acoust. Soc. Am.* **99**, 2055–2066 (1996).
- <sup>22</sup>M. R. Loewen and W. K. Melville, “A model of the sound generated by breaking waves,” *J. Acoust. Soc. Am.* **90**, 2075–2080 (1991).
- <sup>23</sup>G. B. Deane, “Sound generation and air entrainment by breaking waves in the surf zone,” *J. Acoust. Soc. Am.* **102**, 2671–2689 (1997).
- <sup>24</sup>G. B. Deane and M. D. Stokes, “Scale dependence of bubble creation mechanisms in breaking waves,” *Nature Am.* **418**, 839–844 (2002).
- <sup>25</sup>M. J. Buckingham, “On surface-generated ambient noise in an upward refracting ocean,” *Philos. Trans. R. Soc. London* **346**, 321–352 (1994).
- <sup>26</sup>M. J. Buckingham and N. M. Carbone, “Source depth and the spatial coherence of ambient noise in the ocean,” *J. Acoust. Soc. Am.* **102**, 2637–2644 (1997).
- <sup>27</sup>G. B. Deane and M. J. Buckingham, “Vertical coherence of ambient noise in shallow water overlying a fluid seabed,” *J. Acoust. Soc. Am.* **102**, 3413–3424 (1997).
- <sup>28</sup>L. M. Brekhovskikh, *Waves in Layered Media, 2nd ed.* (Academic, New York), pp. 299–305.
- <sup>29</sup>M. J. Buckingham, *Noise in Electronic Devices and Systems* (Ellis Horwood, Chichester, 1983), p. 30.
- <sup>30</sup>L. Ding and D. M. Farmer, “Observations of breaking surface wave statistics,” *J. Phys. Oceanogr.* **24**(6), 1368–1387 (1994).
- <sup>31</sup>I. Tolstoy and C. S. Clay, *Ocean Acoustics: Theory and Experiment in Underwater Sound* (American Institute of Physics, Woodbury, NY), pp. 77, 280–281.